Supporting Information for "Intensification of tropical Pacific biological productivity due to volcanic eruptions"

Megumi O. Chikamoto[1], Axel Timmermann[1], Masakazu Yoshimori[2,3], Flavio Lehner[4,5], Audine Laurian[1], Ayako Abe-Ouchi[3,6], Anne Mouchet[7,8], Fortunat Joos[4], Christoph C. Raible[4], Kim M. Cobb[9]

Corresponding author: Megumi O. Chikamoto, International Pacific Research Center, University of Hawaii, 1680 East-West Road, Honolulu, HI 96817, USA

[1] International Pacific Research Center, University of Hawaii, Honolulu, Hawaii, USA

[2] Faculty of Environmental Earth Science, Hokkaido University, Sapporo, Japan

[3]Atmosphere and Ocean Research Institute, University of Tokyo, Kashiwa, Japan [4]Climate and Environmental Physics, Physics Institute and Oeschger Centre for Climate Change Research, University of Bern, Bern, Switzerland

[5] National Center for Atmospheric Research, Boulder, Colorado, USA

[6] Japan Agency for Marine-Earth Science and Technology, Yokohama, Japan

[7]Laboratoire des Sciences du Climat et de l'Environnement, IPSL-CEA-CNRS-UVSQ, Gif-sur-Yvette, France

[8] Astrophysics and Geophysics Institute, University of Liege, Liege, Belgium

[9]Earth and Atmospheric Sciences, Georgia Institute of Technology, Atlanta, Georgia, USA

Contents of this file

1. Model Description

1.1. MIROC

The MIROC version 3.2 is based on an atmospheric general circulation model with a horizontal spectral truncation T42 (which corresponds to about 2.8° resolution) and 20 vertical sigma levels coupled to an ocean general circulation model with a horizontal resolution of $1.4° \times 0.6°-1.4°$ and 44 vertical levels.

The MIROC Last Millennium simulation (LM-MIROC) uses external forcing of total solar irradiance anomalies derived from three different reconstructions [Crowley, 2000; Bard et al., 2000; Lean et al., 1995] (see description in Table S1 and Figure S1b), volcanic radiative forcing that was specified by using latitude-dependent aerosol optical depth (AOD) anomalies, and greenhouse gas concentrations [Crowley, 2000]. The diagnosed radiative forcing (Figure S1a) is obtained by multiplying AOD by -20 as stated in Gao et al. [2008].

To quantify the marine biogeochemical response to simulated ocean anomalies in MIROC, we additionally use an offline three-dimensional marine biogeochemical model

with a homogenized atmospheric box [Chikamoto et al., 2012]. The box atmosphere in the offline model is only used for calculating the atmospheric carbon dioxide (CO_2) level. The CO_2 level is determined by variations of wind speed, sea surface temperature, sea ice coverage (gas exchange), and sea surface CO_2 concentration (solubility). The biogeochemical model is based on a simplified nutrient-phytoplankton-zooplankton-detritus (NPZD) type. Phytoplankton growth depends on the availability of nitrate concentration and insolation. Detail description of biogeochemical processes is shown in Chikamoto et al. [2012].

The offline biogeochemical model uses daily physical data of ocean velocities, shortwave insolation, temperature, salinity, and sea-ice distribution interpolated from MIROC's monthly outputs. Since this offline method neglects an effect of high frequency physical variability (on timescale shorter than a month), the simulated marine ecosystem response may be slightly different with the simulation obtained from fully coupled Earth System model. However, this difference would be small, which doesn't affect our conclusion on the basis of annual-mean analysis. In our offline approach we do not allow the prognostic atmospheric CO_2 concentration to influence the atmospheric radiation.

The ocean biogeochemical model is spun up for 5000 years using prescribed atmospheric CO_2 of 278 ppmv (corresponding to the level in 850 C.E.) and using monthly physical fields corresponding to the 850 C.E. conditions from the LM-MIROC simulation. After 5000-yr integration, the global-mean dissolved inorganic carbon concentration reaches a steady state, which suggests that the ocean carbon cycle reaches equilibrium. Starting from this steady-state biogeochemical field, we integrate the biogeochemical model with

fully prognostic atmospheric CO_2 from 850 to 1850 C.E. using monthly climate output fields from LM-MIROC.

1.2. CESM

The Community Earth System Model 1.0.1 (CESM; Hurrell et al. [2013]) includes fully-coupled components of the atmosphere, ocean, sea ice, and land surface. The atmosphere component (Community Atmosphere Model 4; Neale et al. [2010]) has a finite volume core with a horizontal resolution of $1.25^\circ \times 0.9^\circ$ and 26 vertical levels. The ocean component is the Parallel Ocean Program version 2 (POP2; Smith et al. [2010]; Danabasoglu et al. [2012]) with a nominal 1° horizontal resolution and 60 levels. The horizontal resolution varies and is higher around the equator for an improved representation of equatorial upwelling. Embedded in POP2 is the Biogeochemical Elemental Cycle model (BEC; Moore et al. [2004]).

The BEC biogeochemical model includes four nutrients (nitrate, phosphate, silicate, and dissolved iron), three phytoplankton functional groups (small phytoplankton, diatoms, and diazotrophs), one zooplankton group, dissolved inorganic and organic carbon, alkalinity and oxygen [Moore et al., 2004; Moore and Braucher, 2008]. River discharge from Community Land Model version 4.0 (CLM4) does not carry dissolved tracers, but prescribed nitrogen deposition at the ocean surface is using the 1850 C.E. data [Lamarque et al., 2010]. In a preindustrial control run in CESM 1.0.3 version, small phytoplankton growth at the tropical Pacific region is determined by the availability of iron, nitrate, insolation, and temperature, while that of diatom is additionally affected by silicate con-

centrations [Chikamoto et al., 2015]. The detail biogeochemical process in the model is described in Moore et al. [2004]; Moore and Braucher [2008].

The last millennium simulation LM-CESM is described in detail in Lehner et al. [2015]. We calculated a 258-year-long 850 C.E. control simulation with CCSM4 [Gent et al., 2011]. Using this steady-state field of the 850 C.E. control simulation, we additionally ran a long 1850 C.E. control simulation. The applied transient forcing largely follows the protocols of PMIP3 [Schmidt et al., 2011]. In particular, we used the variations in AOD due to the volcanic forcing [Gao et al., 2008] (Figure S1a), land use changes [Pongratz et al., 2008], and fossil fuel emissions (post 1750 C.E., following Andres et al. [2012]) (Table S1). Total solar insolation is based on Vieira and Solanki [2010], but was scaled the amplitude of change from the Maunder Minimum to present day by 0.2 % [Keller et al., 2015]. Small drifts in deep-ocean carbon and temperature indicate the not-equilibrated nature of the control simulation. However, there are no detectable drifts in the top 150 meters.

1.3. LOVECLIM

The intermediate complexity model LOVECLIM is based on the ECBilt atmosphere model with a T21 spectral truncation (corresponding to about 5.6° horizontal resolution) and three vertical levels coupled to the ocean-sea ice model CLIO with 3° × 3° horizontal resolution and 20 vertical levels, which is coupled to a thermodynamic-dynamic sea ice model [Goosse et al., 2010]. Allowing for shortwave feedbacks, our version of LOVECLIM adopts a new empirical cloud scheme, which calculates vertically integrated grid-box cloudiness as a function of vertical velocity at 500 hPa, surface temperature, relative humidity, and precipitation [Sriver et al., 2014]. Using annual-mean values of

temperature and precipitation, the vegetation model VECODE computes the evolution of vegetation once a year.

In the three-dimensional global carbon cycle model LOCH, the biogeochemical components are phosphate, silicate, organic matters, and dissolved oxygen [Menviel et al., 2008]. Phytoplankton growth is determined by the availability of phosphate concentration and insolation, and in polar region the growth rate additionally exhibits the temperature dependence. Further description of the biogeochemical model is available in Menviel et al. [2008].

LOVECLIM is integrated for 5000 years with prescribed atmospheric CO_2 of 278 ppmv until reaching a steady-state value, then by prognostic atmospheric CO_2 for 2000 years. We added the forcing of global CO_2 emission after 1751 C.E. due to fossil-fuel burning, cement manufacture and gas flaring from Carbon Dioxide Information Analysis Center (`http://cdiac.ornl.gov/ftp/trends/co2_emis/vir.dat`).

We conducted a 10-member ensemble simulation starting 0 C.E. with different initial conditions until 2000 C.E.. The spin-up period is for 850 years from 0 to 850 C.E., which is enough to reach steady state of the surface dynamics and biogeochemistry. Then we analyzed 10 members of the last millennium simulation from 850 to 1850 C.E.. The ensemble mean provides a more robust estimation of the forced signal component.

References

Andres, R. J., et al., 2012: A synthesis of carbon dioxide emissions from fossil-fuel combustion. *Biogeosciences*, **9**, 1845–1871, doi:10.5194/bg-9-1845-2012.

Bard, E., G. Raisbeck, F. Yiou, and J. Jouzel, 2000: Solar irradiance during the last 1200 years based on cosmogenic nuclides. *Tellus B*, **52 (3)**, 985–992, doi:10.1034/j.1600-0889.2000.d01-7.x.

Chikamoto, M. O., A. Abe-Ouchi, A. Oka, R. Ohgaito, and A. Timmermann, 2012: Quantifying the ocean's role in glacial CO_2 reductions. *Climate of the Past*, **8 (2)**, 545–563, doi:10.5194/cp-8-545-2012.

Chikamoto, M. O., A. Timmermann, Y. Chikamoto, H. Tokinaga, and N. Harada, 2015: Mechanisms and predictability of multiyear ecosystem variability in the North Pacific. *Global Biogeochemical Cycles*, **29**, 2001–2019, doi:10.1002/2015GB005096.

Church, J. A., N. J. White, and J. M. Arblaster, 2005: Significant decadal-scale impact of volcanic eruptions on sea level and ocean heat content. *Nature*, **438 (7064)**, 74–77, doi:10.1038/nature04237.

Crowley, T. J., 2000: Causes of climate change over the past 1000 years. *Science*, **289 (5477)**, 270–277, doi:10.1126/science.289.5477.270.

Danabasoglu, G., S. C. Bates, B. P. Briegleb, S. R. Jayne, M. Jochum, W. G. Large, S. Peacock, and S. G. Yeager, 2012: The CCSM4 ocean component. *Journal of Climate*, **25 (5)**, 1361–1389, doi:10.1175/JCLI-D-11-00091.1.

Gao, C., A. Robock, and C. Ammann, 2008: Volcanic forcing of climate over the past 1500 years: An improved ice core-based index for climate models. *Journal of Geophysical*

Research: Atmospheres, **113**, D23 111, doi:10.1029/2008JD010239.

Gent, P. R., et al., 2011: The community climate system model version 4. *Journal of Climate*, **24 (19)**, 4973–4991, doi:10.1175/2011JCLI4083.1.

Goosse, H., et al., 2010: Description of the earth system model of intermediate complexity LOVECLIM version 1.2. *Geoscientific Model Development*, **3 (2)**, 603–633, doi:10.5194/gmd-3-603-2010.

Houghton, R. A., 2003: Revised estimates of the annual net flux of carbon to the atmosphere from changes in land use and land management 1850–2000. *Tellus B*, **55 (2)**, 378–390, doi:10.1034/j.1600-0889.2003.01450.x.

Hurrell, J. W., et al., 2013: The Community Earth System Model: A Framework for Collaborative Research. *Bulletin of the American Meteorological Society*, **94 (9)**, 1339–1360, doi:10.1175/BAMS-D-12-00121.1.

Keller, K. M., F. Joos, F. Lehner, and C. C. Raible, 2015: Detecting changes in marine responses to ENSO from 850 to 2100 CE: Insights from the ocean carbon cycle. *Geophysical Research Letters*, **42**, 518–525, doi:10.1002/2014GL062398.

Lamarque, J.-F., et al., 2010: Historical (1850–2000) gridded anthropogenic and biomass burning emissions of reactive gases and aerosols: Methodology and application. *Atmospheric Chemistry and Physics*, **10 (15)**, 7017–7039, doi:10.5194/acp-10-7017-2010.

Lean, J., J. Beer, and R. Bradley, 1995: Reconstruction of solar irradiance since 1610: Implications for climate change. *Geophysical Research Letters*, **22 (23)**, 3195–3198, doi:10.1029/95GL03093.

Lehner, F., F. Joos, C. C. Raible, J. Mignot, A. Born, K. M. Keller, and T. F. Stocker, 2015: Climate and carbon cycle dynamics in a CESM simulation from 850 to 2100 CE. *Earth System Dynamics*, **6 (2)**, 411–434, doi:10.5194/esd-6-411-2015.

Masson-Delmotte, V., et al., 2013: Information from paleoclimate archives. *Climate change*, 383–464.

Menviel, L., A. Timmermann, A. Mouchet, and O. Timm, 2008: Meridional reorganizations of marine and terrestrial productivity during Heinrich events. *Paleoceanography*, **23 (1)**, PA1203, doi:10.1029/2007PA001445.

Moore, J. and O. Braucher, 2008: Sedimentary and mineral dust sources of dissolved iron to the world ocean. *Biogeosciences*, **5 (3)**, 631–656, doi:10.5194/bg-5-631-2008.

Moore, J. K., S. C. Doney, and K. Lindsay, 2004: Upper ocean ecosystem dynamics and iron cycling in a global three-dimensional model. *Global Biogeochemical Cycles*, **18 (4)**, GB4028, doi:10.1029/2004GB002220.

Muscheler, R., F. Joos, J. Beer, S. A. Müller, M. Vonmoos, and I. Snowball, 2007: Solar activity during the last 1000 yr inferred from radionuclide records. *Quaternary Science Reviews*, **26**, 82–97, doi:10.1016/j.quascirev.2006.07.012.

Neale, R. B., et al., 2010: *Description of the NCAR community atmosphere model (CAM 5.0). NCAR Tech. Note NCAR/TN-486+ STR.*

Pongratz, J., C. Reick, T. Raddatz, and M. Claussen, 2008: A reconstruction of global agricultural areas and land cover for the last millennium. *Global Biogeochemical Cycles*, **22**, GB3018, doi:10.1029/2007GB003153.

Rayner, N., D. E. Parker, E. Horton, C. Folland, L. Alexander, D. Rowell, E. Kent, and A. Kaplan, 2003: Global analyses of sea surface temperature, sea ice, and night marine air temperature since the late nineteenth century. *Journal of Geophysical Research: Atmospheres*, **108 (D14)**, 4407, doi:10.1029/2002JD002670.

Schmidt, G., et al., 2011: Climate forcing reconstructions for use in PMIP simulations of the last millennium (v1. 0). *Geoscientific Model Development*, **4 (1)**, 33–45, doi:10.5194/gmd-4-33-2011.

Smith, R., et al., 2010: The Parallel Ocean Program (POP) Reference Manual Ocean Component of the Community Climate System Model (CCSM) and Community Earth System Model (CESM). *Rep. LAUR-01853*, **141**.

Sriver, R. L., A. Timmermann, M. E. Mann, K. Keller, and H. Goosse, 2014: Improved representation of tropical Pacific Ocean–atmosphere dynamics in an intermediate complexity climate model. *Journal of Climate*, **27 (1)**, 168–185, doi:10.1175/JCLI-D-12-00849.1.

Stenchikov, G., T. L. Delworth, V. Ramaswamy, R. J. Stouffer, A. Wittenberg, and F. Zeng, 2009: Volcanic signals in oceans. *Journal of Geophysical Research: Atmospheres*, **114**, D16 104, doi:10.1029/2008JD011673.

Vieira, L. E. A. and S. K. Solanki, 2010: Evolution of the solar magnetic flux on time scales of years to millenia. *Astronomy & Astrophysics*, **509**, A100, doi:10.1051/0004-6361/200913276.

Table S1. External forcing of the last millennium simulations

Model	Orbital	Solar irradiance	Trace gasses	Volcanoes	Land Use
MIROC	PMIP3[1]	PMIP3 (CBL*)	PMIP3[1]	Gao et al. [2008][4]	–
CESM	PMIP3[1]	PMIP3[1] (Vieira and Solanki [2010])	PMIP3[1] (1751CE ∼) Andres et al. [2012]	Gao et al. [2008][4]	PMIP3 (Pongratz et al. [2008][5])
LOVECLIM	PMIP3[1]	PMIP3 (Muscheler et al. [2007][7])	(1751CE ∼) CDIAC[6]	Crowley [2000][8]	(1850CE ∼) Houghton [2003][9]

(*) CBL is spliced data set of Crowley [2000][1], Bard et al. [2000][2], Lean et al. [1995][3]. Since the Crowley data cover only after 1000 CE, we fit a spline to the data from the Crowley data to the Bard data. Then the resulting time series were scaled to the Lead data that cover only 1610 CE onward. The final scaling was performed to become consistent with the solar forcing in the MIROC's 20th century historical run submitted to CMIP3.

Data are available at

(1) http://www.ncdc.noaa.gov/paleo/pubs/crowley.html
(2) ftp://ftp.ncdc.noaa.gov/pub/data/paleo/climate_forcing/solar_variability/bard_irradiance.txt
(3) ftp://ftp.ncdc.noaa.gov/pub/data/paleo/climate_forcing/solar_variability/lean2000_irradiance.txt
(4) http://climate.envsci.rutgers.edu/IVI2/
(5) http://cera-www.dkrz.de/WDCC/ui/Compact.jsp?acronym=RECON_LAND_COVER_800-1992
(6) http://cdiac.esd.ornl.gov/ftp/ndp030/global.1751_2008.ems
(7) ftp://ftp.ncdc.noaa.gov/pub/data/paleo/climate_forcing/solar_variability/muscheler2007solar-mod.txt
(8) ftp://ftp.ncdc.noaa.gov/pub/data/paleo/gcmoutput/crowley2000/
(9) http://cdiac.ornl.gov/trends/landuse/houghton/houghton.html

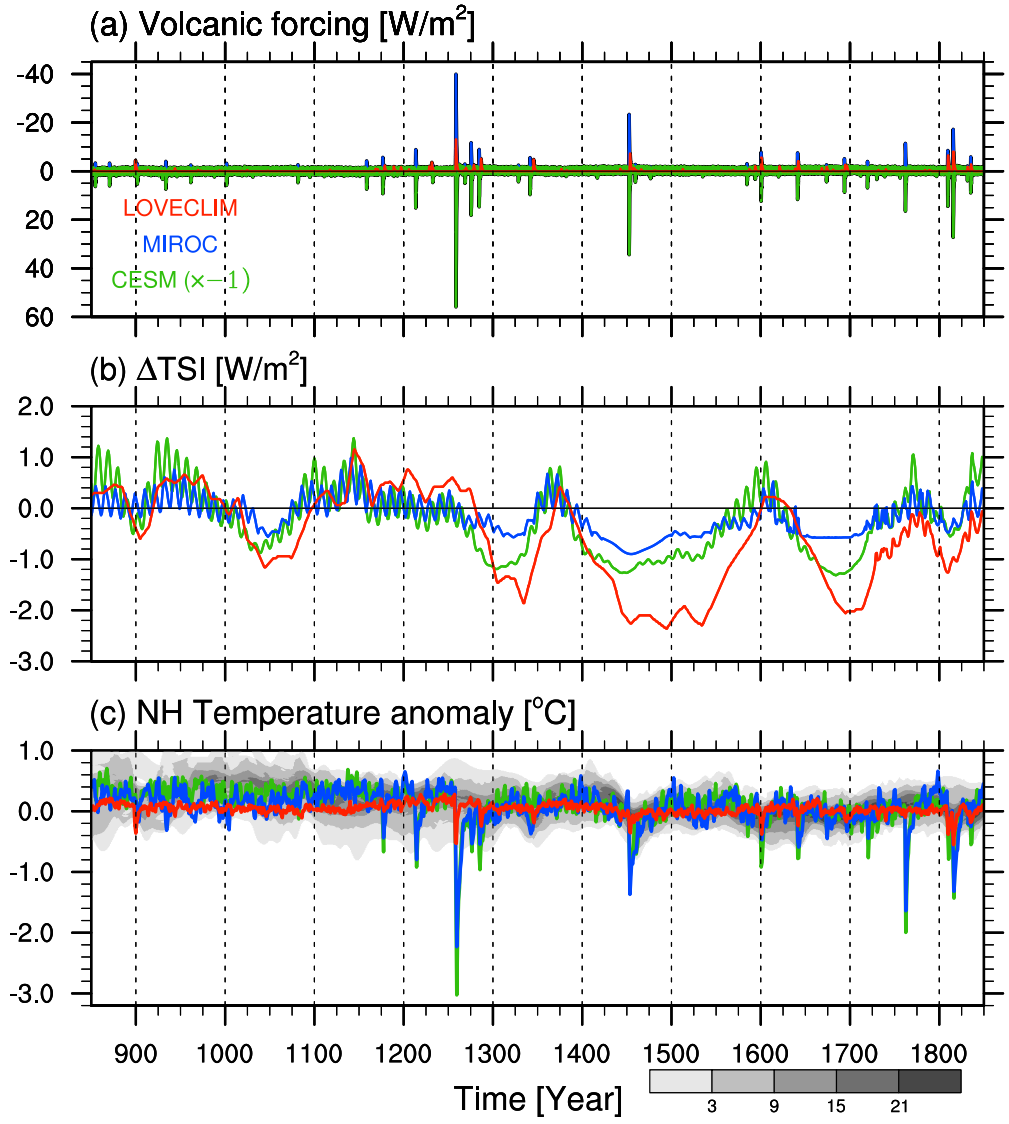

Figure S1. Time series of monthly-mean (a) volcanic forcing of MIROC (blue) [Gao et al., 2008], CESM (green) [Gao et al., 2008], and LOVECLIM (red) [Crowley, 2000], annual-mean (b) solar irradiance forcing, and (c) atmospheric 2m temperature anomaly in the Northern Hemisphere for the 1500 to 1850 reference periods, and the concentration of overlapping NH temperature reconstructions for the 1500 to 1850 reference period (in Figure 5.8 by IPCC AR5 [Masson-Delmotte et al., 2013]) (grey shading).

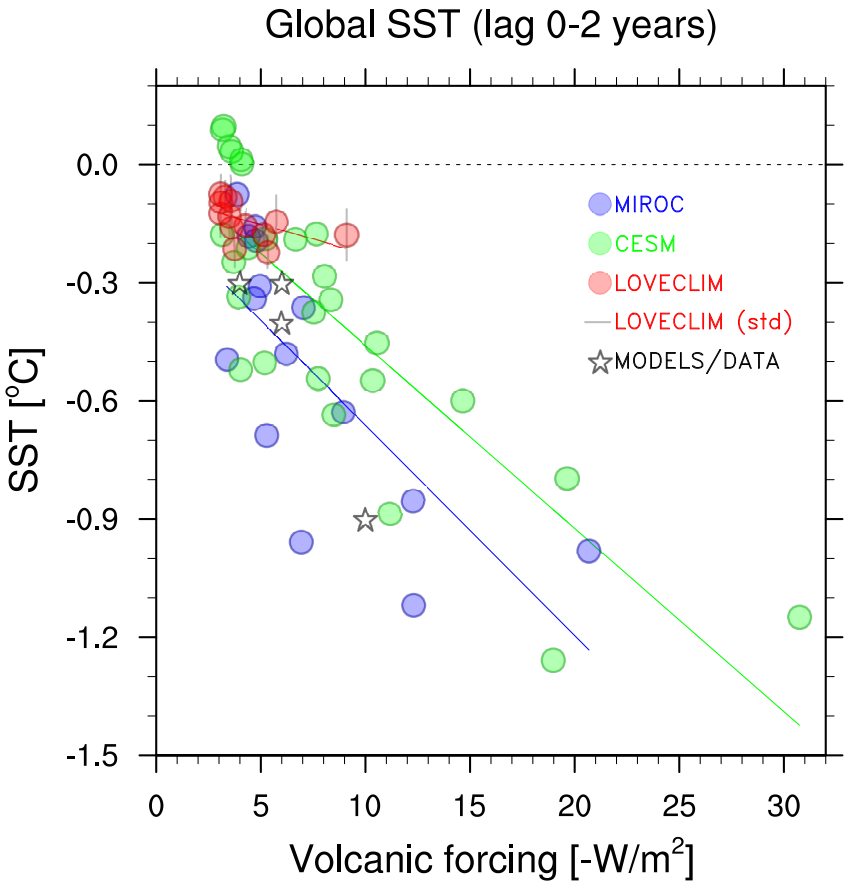

Figure S2. Scatter plots of volcanic forcing ($-$ W m^{-2}) and the anomaly of global SST (°C) with 0–2 years mean lag from the 1000-year mean in MIROC (blue circles), CESM (green circles) and LOVECLIM ensemble mean (red circles). Black stars show the global-mean SST estimates in another model [Church et al., 2005; Stenchikov et al., 2009] or historical SST analysis studies [Rayner et al., 2003]. Grey lines are standard deviation of 10 ensemble members in LOVECLIM. Blue, green and red lines are the regression between the volcanic forcing and the SST change in each model.

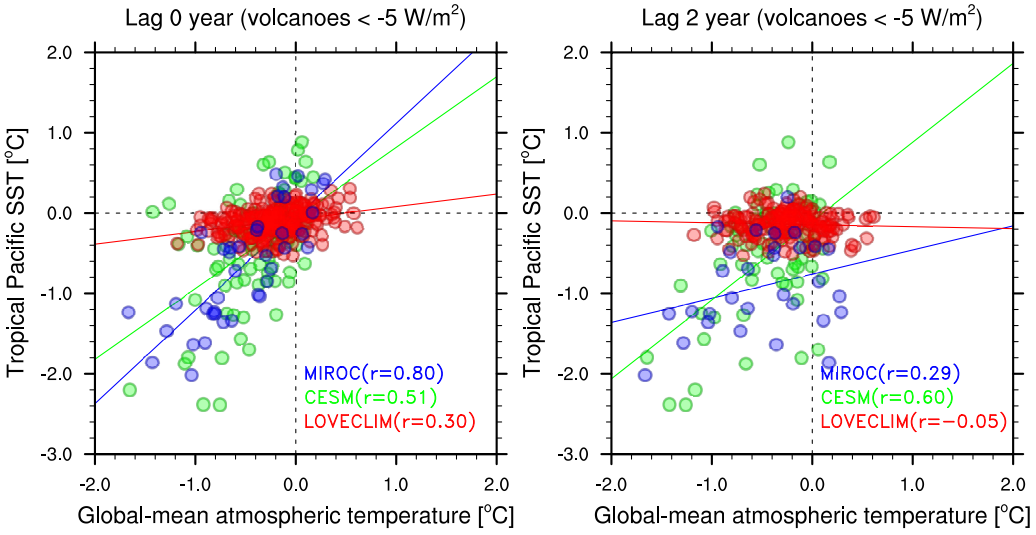

Figure S3. Scatter plots of the anomalies of global-mean atmospheric 2m temperature (°C) and of the tropical Pacific SST (°C) (5°S–5°N, 120°E–80°W) with lag 0 and 2 years (for the period from −2 to +5 years) after strong volcanic events (< −5 W m^{-2}) in MIROC (blue), CESM (green), and LOVECLIM (with all ensemble members, red). In the left figure with lag 0 year (for 8-year analysis), it exhibits 40 cases for 5 volcanic events (= 5 events × 8 years) in MIROC, 88 cases for 11 volcanic events in CESM, and 240 cases for 3 volcanic events in LOVECLIM. In the right figure with lag 2 years (for 6-year analysis), it includes 30 cases in MIROC, 66 cases in CESM, and 180 cases in LOVECLIM.